

Absolute branching fraction measurements for exclusive D_s semileptonic decays

J. Yelton,¹ P. Rubin,² N. Lowrey,³ S. Mehrabyan,³ M. Selen,³ J. Wiss,³ R. E. Mitchell,⁴ M. R. Shepherd,⁴ D. Besson,⁵ T. K. Pedlar,⁶ D. Cronin-Hennessy,⁷ K. Y. Gao,⁷ J. Hietala,⁷ Y. Kubota,⁷ T. Klein,⁷ R. Poling,⁷ A. W. Scott,⁷ P. Zweber,⁷ S. Dobbs,⁸ Z. Metreveli,⁸ K. K. Seth,⁸ B. J. Y. Tan,⁸ A. Tomaradze,⁸ J. Libby,⁹ L. Martin,⁹ A. Powell,⁹ G. Wilkinson,⁹ H. Mendez,¹⁰ J. Y. Ge,¹¹ D. H. Miller,¹¹ V. Pavlunin,¹¹ B. Sanghi,¹¹ I. P. J. Shipsey,¹¹ B. Xin,¹¹ G. S. Adams,¹² D. Hu,¹² B. Moziak,¹² J. Napolitano,¹² K. M. Ecklund,¹³ Q. He,¹⁴ J. Insler,¹⁴ H. Muramatsu,¹⁴ C. S. Park,¹⁴ E. H. Thorndike,¹⁴ F. Yang,¹⁴ M. Artuso,¹⁵ S. Blusk,¹⁵ S. Khalil,¹⁵ J. Li,¹⁵ R. Mountain,¹⁵ K. Randrianarivony,¹⁵ N. Sultana,¹⁵ T. Skwarnicki,¹⁵ S. Stone,¹⁵ J. C. Wang,¹⁵ L. M. Zhang,¹⁵ G. Bonvicini,¹⁶ D. Cinabro,¹⁶ M. Dubrovin,¹⁶ A. Lincoln,¹⁶ M. J. Smith,¹⁶ P. Naik,¹⁷ J. Rademacker,¹⁷ D. M. Asner,¹⁸ K. W. Edwards,¹⁸ J. Reed,¹⁸ A. N. Robichaud,¹⁸ G. Tatishvili,¹⁸ E. J. White,¹⁸ R. A. Briere,¹⁹ H. Vogel,¹⁹ P. U. E. Onyisi,²⁰ J. L. Rosner,²⁰ J. P. Alexander,²¹ D. G. Cassel,²¹ J. E. Duboscq,^{21,*} R. Ehrlich,²¹ L. Fields,²¹ L. Gibbons,²¹ R. Gray,²¹ S. W. Gray,²¹ D. L. Hartill,²¹ B. K. Heltsley,²¹ D. Hertz,²¹ J. M. Hunt,²¹ J. Kandaswamy,²¹ D. L. Kreinick,²¹ V. E. Kuznetsov,²¹ J. Ledoux,²¹ H. Mahlke-Krüger,²¹ D. Mohapatra,²¹ J. R. Patterson,²¹ D. Peterson,²¹ D. Riley,²¹ A. Ryd,²¹ A. J. Sadoff,²¹ X. Shi,²¹ S. Stroiney,²¹ W. M. Sun,²¹ and T. Wilksen²¹

(CLEO Collaboration)

¹University of Florida, Gainesville, Florida 32611, USA²George Mason University, Fairfax, Virginia 22030, USA³University of Illinois, Urbana-Champaign, Illinois 61801, USA⁴Indiana University, Bloomington, Indiana 47405, USA⁵University of Kansas, Lawrence, Kansas 66045, USA⁶Luther College, Decorah, Iowa 52101, USA⁷University of Minnesota, Minneapolis, Minnesota 55455, USA⁸Northwestern University, Evanston, Illinois 60208, USA⁹University of Oxford, Oxford OX1 3RH, UK¹⁰University of Puerto Rico, Mayaguez, Puerto Rico 00681¹¹Purdue University, West Lafayette, Indiana 47907, USA¹²Rensselaer Polytechnic Institute, Troy, New York 12180, USA¹³Rice University, Houston, Texas 77005, USA¹⁴University of Rochester, Rochester, New York 14627, USA¹⁵Syracuse University, Syracuse, New York 13244, USA¹⁶Wayne State University, Detroit, Michigan 48202, USA¹⁷University of Bristol, Bristol BS8 1TL, UK¹⁸Carleton University, Ottawa, Ontario, Canada K1S 5B6¹⁹Carnegie Mellon University, Pittsburgh, Pennsylvania 15213, USA²⁰University of Chicago, Chicago, Illinois 60637, USA²¹Cornell University, Ithaca, New York 14853, USA

(Received 3 March 2009; published 18 September 2009)

We measure the absolute branching fractions of D_s semileptonic decays where the hadron in the final state is one of ϕ , η , η' , K_S^0 , K^{*0} , and f_0 , using $2.8 \times 10^5 e^+e^- \rightarrow D_s D_s^*$ decays collected in the CLEO-c detector at a center-of-mass energy close to 4170 MeV. We obtain $\mathcal{B}(D_s^+ \rightarrow \phi e^+ \nu_e) = (2.29 \pm 0.37 \pm 0.11)\%$, $\mathcal{B}(D_s^+ \rightarrow \eta e^+ \nu_e) = (2.48 \pm 0.29 \pm 0.13)\%$, $\mathcal{B}(D_s^+ \rightarrow \eta' e^+ \nu_e) = (0.91 \pm 0.33 \pm 0.05)\%$, where the first uncertainties are statistical and the second are systematic. We also obtain $\mathcal{B}(D_s^+ \rightarrow K^0 e^+ \nu_e) = (0.37 \pm 0.10 \pm 0.02)\%$, and $\mathcal{B}(D_s^+ \rightarrow K^{*0} e^+ \nu_e) = (0.18 \pm 0.07 \pm 0.01)\%$, which are the first measurements of Cabibbo suppressed exclusive D_s semileptonic decays, and, $\mathcal{B}(D_s^+ \rightarrow f_0 e^+ \nu_e) \times \mathcal{B}(f_0 \rightarrow \pi^+ \pi^-) = (0.13 \pm 0.04 \pm 0.01)\%$. This is the first absolute product branching fraction determination for a semileptonic decay including a scalar meson in the final state.

DOI: 10.1103/PhysRevD.80.052007

PACS numbers: 13.20.Fc

*Deceased

The study of D_s semileptonic decays provides interesting information on several aspects of heavy quark decays. First of all, the total semileptonic width provides discrimination between different theoretical evaluations of had-

ronic matrix elements affecting charm semileptonic decays. The Operator Product Expansion (OPE) predicts that all the charmed mesons have the same semileptonic width, modulo nonfactorizable corrections [1]. The ISGW2 form factor model [2] predicts a difference between the D and D_s inclusive rates, as the spectator quark masses m_u and m_s differ on the scale of the daughter quark mass m_s in the Cabibbo favored semileptonic transition. The D^+ and D^0 semileptonic widths are equal within the 3% accuracy of the measurements, and the compositions of their inclusive spectra are dominated by the lowest lying resonances [3]. This result is explained by the observation that the s quark in the final state is usually produced with a small enough momentum to be bound to the spectator antiquark in an $l=0$ $s\bar{q}$ meson [4]. D_s semileptonic decays share these kinematic features, and thus an absolute measurement of D_s semileptonic decays sheds some light also on inclusive processes. Specific decays contribute valuable information on light meson properties. For example, the fraction of semileptonic decays going into η and η' is sensitive to the pseudoscalar mixing angle, and may indeed shed some light on $\eta - \eta'$ -glueball mixing [5]. In addition, decays including $\pi\pi$ and KK in the final state can elucidate the nature of exotic light scalar mesons [6,7].

D_s exclusive semileptonic decays have been studied by ARGUS, CLEO, BaBar, and fixed target experiments. No absolute measurements of branching fractions exist. The branching fraction $D_s^+ \rightarrow \phi \ell^+ \nu_\ell$, which is the most widely studied [8–12], is generally normalized with respect to the decay $D_s \rightarrow \phi \pi$. However, the Dalitz plot for this mode shows the presence of a significant broad scalar resonance whose contribution to the observed yields changes depending upon the selection criteria [13]. For this reason, this mode is not suitable for normalization. Recently, the BABAR collaboration [14] used the normalization mode $D_s \rightarrow KK\pi$ with a mass cut of ± 10 MeV around the nominal ϕ as suggested in Ref. [13], to obtain $\mathcal{B}(D_s^+ \rightarrow \phi e^+ \nu_e) = (2.61 \pm 0.03 \pm 0.08 \pm 0.15)\%$. CLEO measured [15] the ratio $[\Gamma(\eta \ell^+ \nu_\ell) + \Gamma(\eta' \ell^+ \nu_\ell)]/[\Gamma(\phi \ell^+ \nu_\ell)] = 1.67 \pm 0.17 \pm 0.17$. Finally, BES [16] reported the inclusive branching fraction $\mathcal{B}(D_s^+ \rightarrow e^+ \text{ anything}) = (7.7^{+5.7+2.4}_{-4.3-2.1})\%$. The uncertainties are too large to allow a meaningful comparison between inclusive and exclusive channels.

We use a data sample of 310 pb^{-1} , collected at a center-of-mass (CM) energy close to 4170 MeV, with the CLEO-c detector [17,18]. The momenta and directions of charged particles are reconstructed in the tracking system, which also provides charged particle identification information based on specific ionization (dE/dx). A Ring Imaging Cherenkov Detector (RICH) completes the charged particle identification system [19], and is critical near 1 GeV, where the specific ionization bands of the K and π overlap. The photon energy and direction are measured in the CsI

electromagnetic calorimeter, whose energy measurement E , combined with the momentum p information from the tracking system, provides the key electron identification variable E/p . The CsI calorimeter measures the electron and photon energies with an r.m.s. resolution of 2.2% at $E = 1$ GeV and 5% at $E = 100$ MeV.

At $E_{\text{CM}} = 4170$ MeV, the cross section for e^+e^- annihilation into $D_s^{*+}D_s^- + D_s^+D_s^{*-}$ is approximately 0.9 nb, while other charm production totals ~ 7 pb, and the light quark continuum cross section is ~ 12 nb [20]. We look for semileptonic decays of the D_s^+ in events in which the D_s^- is fully reconstructed in a hadronic mode (tagged events). Each event also must include at least one isolated photon, as either the D_s^+ or D_s^- originates from a D_s^* . Here and throughout the paper, charge conjugate decays are implied. Charged tracks are used to form the D_s^- if their fitted helical trajectory approaches the event origin within a distance of 5 mm in the azimuthal projection and 5 cm in the polar projection (θ), where the azimuthal projection is in the bend view of the solenoidal magnet. In addition, each track must possess at least 50% of the hits expected, must be within the fiducial volume of the drift chamber, and must have a momentum of at least 40 MeV. Pions and kaons are identified using dE/dx and RICH if their momenta are above 700 MeV, otherwise only dE/dx identification is used. We form η and π^0 candidates from pairs of photons that deposit energy in the calorimeter in a manner consistent with an electromagnetic shower and are not matched to tracks. We require that the two photons to have less than 3σ pull mass which is defined as the standard deviation from the expected π^0 or η mass. In the best calorimeter region ($|\cos\theta| < 0.71$) we use photons with energies greater than 30 MeV, while in the endcap region ($0.93 > |\cos\theta| > 0.85$) we require an energy greater than 50 MeV.

The tag modes used are listed in Table I. Some tag specific selection criteria are applied. For the modes $D_s^- \rightarrow K^+K^-\pi^-$ and $D_s^- \rightarrow K^+K^-\pi^-\pi^0$, the π is required to have a momentum greater than 100 MeV to suppress the background from D^* decays. Similarly, for the mode $D_s^- \rightarrow \pi^+\pi^-\pi^-$, two pions of opposite charge must have momentum greater than 100 MeV. The Charged track pairs used to reconstruct K_S^0 (via $K_S^0 \rightarrow \pi^+\pi^-$) are required to have an invariant mass within 3σ of the K_S^0 mass. In addition, for the $D_s^- \rightarrow K_S^0K^-$ and $D_s^- \rightarrow K^{*-}K^0$ tags, we require candidate K_S^0 to originate from a vertex displaced from the interaction point, and the K_S^0 momentum vector, obtained from a kinematic fit of the charged π momenta, must point back to the beam spot. For resonance decays we select intervals in invariant mass centered on the resonance masses [21] and within ± 150 MeV for $\rho^- \rightarrow \pi^-\pi^0$, ± 100 MeV for $K^* \rightarrow K\pi$, ± 10 MeV for $\eta' \rightarrow \eta\pi^+\pi^-$ or $\eta' \rightarrow \rho\gamma$. In addition, for the latter η' decay mode, we apply a helicity angle cut which is the angle measured in the rest frame of the decay-

TABLE I. Tagging modes and number of signal and background (Bkg) events, determined from two-Gaussian fits to the invariant mass distributions. The signal window is $\pm 2.5\sigma$ of the D_s^- mass for all modes, except $\eta\rho^-$ ($\pm 2\sigma$). The last two columns show the corresponding estimates of the number signal and background tags accompanied by a reconstructed γ from $D_s^* \rightarrow \gamma D_s$ transition, which are determined from the MM^{*2} spectrum (see text).

Mode	Invariant Mass		MM^{*2}	
	Signal	Bkg	Signal	Bkg
$K^+ K^- \pi^-$	13952 ± 232	11280	8245 ± 245	13970
$K_S^0 K^-$	2943 ± 128	561	1749 ± 146	1555
$\eta \pi^-$	1806 ± 120	4747	1241 ± 123	3936
$\eta'(\eta \pi^+ \pi^-) \pi^-$	1231 ± 55	415	907 ± 109	1036
$K^- K^+ \pi^- \pi^0$	5300 ± 401	34419	2913 ± 289	24985
$\pi^+ \pi^- \pi^-$	4331 ± 716	25824	2439 ± 558	16619
$K^{*0} K^0$	1565 ± 114	1442	841 ± 87	2440
$\eta \rho^-$	4002 ± 254	22044	2168 ± 268	18450
$\pi^- \eta'(\rho \gamma)$	2515 ± 342	18593	1817 ± 212	12061
Sum	37645 ± 978	119325	22320 ± 792	95052

ing parent particle between the direction of the decay daughter and the direction of the grandparent particle as $|\cos\theta_\pi| < 0.8$. Tags are required to have momentum consistent with coming from $D_s D_s^*$ decay.

We further select tags using the recoiling mass M_{rec} ,

$$M_{\text{rec}} = \sqrt{(E_{\text{CM}} - E_{D_s^-})^2 - (\mathbf{p}_{\text{CM}} - \mathbf{p}_{D_s^-})^2}, \quad (1)$$

where E_{CM} (\mathbf{p}_{CM}) is the CM energy (momentum), E_{D_s} (\mathbf{p}_{D_s}) is the tag energy (momentum). D_s^* daughter tags peak broadly in M_{rec} due to the presence of the photon in the tag side, while directly produced D_s^- tags have a narrow peak. We accept events for which M_{rec} is within $-55 \text{ MeV} \leq M_{\text{rec}} - M_{D_s^*} < 55 \text{ MeV}$. This cut is broad enough to encompass both the narrow peak associated with D_s tags and almost all the broad component associated with tags that originate from D_s^* . Then we fit the invariant mass distribution M_{D_s} of these events, using a two-Gaussian shape for the signal plus a polynomial background shape. The signal component allows us to define an effective $\sigma = f_1 \sigma_1 + (1 - f_1) \sigma_2$ where σ_1 and σ_2 are the standard deviations of the two Gaussian components and f_1 is the fractional area of the first Gaussian. We require that the candidate invariant mass to be within 2.5σ (2σ for the $\eta\rho$ mode) of the nominal D_s mass [21]. Random D_s backgrounds are estimated through sideband samples. We then combine the tag with a well reconstructed γ and calculate the missing mass squared MM^{*2} , the square of the invariant mass of the system recoiling against the γ -tag pair.

$$MM^{*2} = (E_{\text{CM}} - E_{D_s^-} - E_\gamma)^2 - (\mathbf{p}_{\text{CM}} - \mathbf{p}_{D_s^-} - \mathbf{p}_\gamma)^2, \quad (2)$$

where E_γ (\mathbf{p}_γ) is the energy (momentum) of the additional γ . In order to improve the MM^{*2} resolution, we use a kinematic fit that constrains the D_s decay products to M_{D_s} and conserves overall momentum and energy.

Figure 1 shows the MM^{*2} distribution for the nine tags considered. In order to estimate the number of tags used for further analysis, we use a two-dimensional binned maximum likelihood fit of the measured MM^{*2} and M_{D_s} distributions. We consider three components in the fit: a signal, comprising true tags accompanied by the photon from the D_s^* , a background composed by true tags combined with a random photon, and a second background comprising false tags. We infer the D_s combinatoric background from two 5σ (4σ for the $\eta\rho$ mode) wide intervals on both sides of the M_{D_s} signal peak. The MM^{*2} signal fit is improved by using a probability distribution function (PDF) derived from fully reconstructed $D_s D_s^*$ events. We fit signal and sideband intervals in M_{D_s} simultaneously. The sideband intervals constrain the shape of the random D_s background. We then extract the tag yield from the fitted signal function integrated within $\pm 2.5\sigma$ around the MM^{*2} most probable value. For the nine modes considered, Table I shows the number of signal and background tags, as well as the signal and background tags reconstructed in conjunction with an isolated photon.

We next describe reconstruction of the semileptonic decays. For any given tag-photon combination, we seek a candidate e^+ and a set of hadrons. Positrons are identified on the basis of a likelihood ratio constructed from three inputs: the ratio between the energy deposited in the calorimeter and the momentum measured in the tracking system, the specific ionization dE/dx measured in the drift chamber, and RICH information [22]. Our selection efficiency averages 0.95 in the momentum region 0.3–1.0 GeV, and 0.71 in the region 0.2–0.3 GeV. The average fractions of charged π and K incorrectly identified as positrons averaged over the relevant momentum range are approximately 0.1%. We study events containing ϕ , η , η' , K_S^0 , K^{*0} , and f_0 in the final state. Track and γ selection criteria, as well as resonance cuts are the same as used in the tag reconstruction except that we select candidates with invariant masses within ± 10 MeV of the known ϕ mass [21] for $\phi \rightarrow K^+ K^-$, and within ± 75 MeV of the known K^{*0} mass for $K^{*0} \rightarrow K^+ \pi^-$. Among the η candidates not used in forming a tag, we choose the one with the smallest pull mass to form $\eta e^+ \nu_e$ and $\eta' e^+ \nu_e$ candidates. We use $\eta' \rightarrow \eta \pi^+ \pi^-$ only. For the channel $K^{*0} \rightarrow K^+ \pi^-$, the K and e must have the same charge. Finally, we form f_0 candidates by combining two pions of opposite charge and require that their invariant mass be within 100 MeV of the known f_0 mass. In each case we require that the event have no unused tracks, and that the tag and semileptonic candidate have opposite charge.

For each γ candidate, we perform two kinematic fits, one assuming that the γ combines with the tag to form a

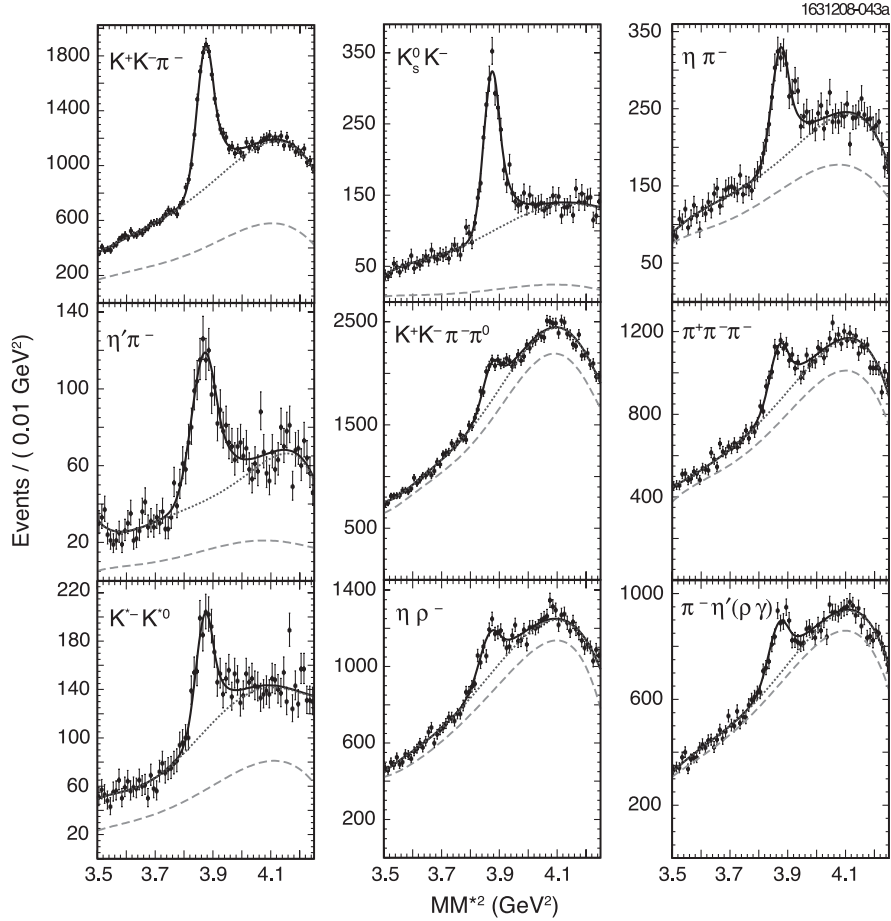


FIG. 1. The MM^2 distribution from events with a photon in addition to the D_s^- tag. In each plot, the D_s^- mode studied is indicated, and the solid curve represents a fit to a Crystal Ball function (signal), the dotted curve represents the total background, and the dashed curve represents the background composed of random D_s tags, constrained by the sideband sample. Both terms are well described by 5th order Chebychev polynomial background functions.

D_s^{*-} , the other assuming that the semileptonic decay comes from a D_s^{*+} parent. We require the $D_s D_s^*$ pair to conserve energy and momentum in the CM frame, and the mass of the candidate D_s to be consistent with the known mass. When we assume the tag to be the daughter of a D_s^{*-} , we constrain the energy of the photon plus tag candidate to be consistent with the expected D_s^{*-} energy, otherwise we constrain the energy of the tag candidate to be consistent with the D_s^- energy in the CM system. Finally we choose the photon and hypothesis with the smallest χ^2 and calculate the missing mass squared MM^2 defined as

$$MM^2 = (E_{CM}^* - E_{D_s^-}^* - E_\gamma^* - E_e^* - E_{had}^*)^2 - (-\mathbf{p}_{D_s^-}^* - \mathbf{p}_\gamma^* - \mathbf{p}_e^* - \mathbf{p}_{had}^*)^2, \quad (3)$$

where $E_e^*(\mathbf{p}_e^*)$ is the energy (momentum) of the positron candidate and $E_{had}^*(\mathbf{p}_{had}^*)$ is the energy (momentum) of the hadron candidate in the CM system. For signal events, MM^2 is the ν_e invariant mass squared and thus it peaks at zero. Figure 2 shows the measured MM^2 for each final state summed over all tag modes used. We require signal

events to have a $|MM^2| < 0.05 \text{ GeV}^2$. We estimate the background coming from random D_s^- tags by studying the sideband samples, and the remaining background by studying a sample of simulated $DD\bar{D}$ events that is 20 times bigger than our data set. Figure 2 shows the signal and background distributions for the six modes studied. The MM^2 shapes are well modeled by the signal Monte Carlo simulation. We show also the background estimates from the sideband data sample, as well as the background predictions from a Monte Carlo simulation of charm meson decays at this center-of-mass energy. Note that the background is small in all the modes considered. We have also investigated backgrounds produced by random photons associated with a true semileptonic event, and we found these to be even smaller, thus we do not subtract them.

We evaluate exclusive branching fractions for semileptonic decays including the hadron i through the relationship

$$B_i \equiv \frac{\sum_\alpha (n_\alpha^i - n_{\alpha, \text{bkg}}^i)}{\epsilon_{\text{SL}}^i (\sum_\alpha n_\alpha) B_i^{\text{had}}} \quad (4)$$

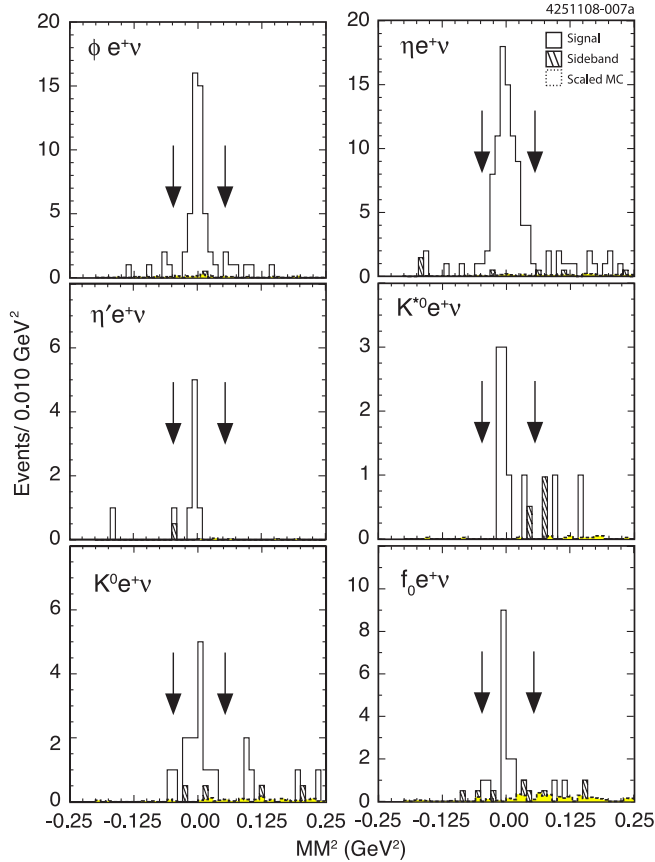


FIG. 2 (color online). The MM^2 distribution for tagged semileptonic events in the exclusive modes: $D_s^+ \rightarrow \phi e^+ \nu_e$, $D_s^+ \rightarrow \eta e^+ \nu_e$, $D_s^+ \rightarrow \eta' e^+ \nu_e$, $D_s^+ \rightarrow K^{*0} e^+ \nu_e$, $D_s^+ \rightarrow K^0 e^+ \nu_e$, and $D_s^+ \rightarrow f_0 e^+ \nu_e$. The solid entries correspond to the events from signal regions, the hatched entries are the events from sideband and the dashed entries represent the scaled background events from generic MC.

where the index α runs over the tag modes, the index i represents a specific hadronic final state, $\mathcal{B}_i^{\text{had}}$ identifies the branching fraction for that state, and ϵ_{SL}^i represents the average efficiency for finding the exclusive semileptonic decay in the tag sample used. We evaluate the semileptonic efficiency by considering two Monte Carlo (MC) samples. The first contains a tag event accompanied by a semileptonic decay (double-tag sample), while the latter contains a tag accompanied by a generic D_s decay (single-tag sample). The ratio of the single and double tag efficiencies is the desired ϵ_{SL} for each tag. Table II shows the signal, and background yields, ϵ_{SL} and the branching fractions determined for the six semileptonic channels. We derive ϵ_{SL} from each tag mode independently, and then we compute their average weighted by tag abundance. The efficiency obtained with this method accounts for the different tag efficiency in semileptonic and generic D_s decays. We treat the exclusive channel $\phi e^+ \nu_e$ slightly differently: as the ϕ reconstruction efficiency is strongly momentum dependent, we perform the analysis in five 200 MeV wide

TABLE II. The signal and background yields, the semileptonic efficiency ϵ_{SL}^i and the derived branching fractions for the six semileptonic channels studied. The $D_s^+ \rightarrow f_0 e^+ \nu_e$ branching fraction quoted represents the product branching fraction $\mathcal{B}(D_s^+ \rightarrow f_0 e^+ \nu_e) \times \mathcal{B}(f_0 \rightarrow \pi^+ \pi^-)$, which is the dominant decay mode in Ref. [21].

Signal Mode	n^i	n_{bkg}^i	ϵ_{SL}^i (%)	\mathcal{B} (%)
$D_s^+ \rightarrow \phi e^+ \nu_e$	45.50	0.06	17.79 ± 0.33	2.29 ± 0.37
$D_s^+ \rightarrow \eta e^+ \nu_e$	82.49	0.32	37.65 ± 0.27	2.48 ± 0.29
$D_s^+ \rightarrow \eta' e^+ \nu_e$	7.50	0.06	21.04 ± 0.22	0.91 ± 0.33
$D_s^+ \rightarrow K^{*0} e^+ \nu_e$	13.99	0.29	33.14 ± 0.26	0.37 ± 0.10
$D_s^+ \rightarrow K^0 e^+ \nu_e$	7.50	0.18	27.52 ± 0.23	0.18 ± 0.07
$D_s^+ \rightarrow f_0 e^+ \nu_e$	13.99	0.88	46.79 ± 0.31	0.13 ± 0.04

momentum bins. We attribute all the signal events in the $K^+ K^- e^+ \nu_e$ in the final state to form the $\phi e \nu_e$ channel. Recent BaBar studies [14] have estimated the S -wave fraction to be $(0.22_{-0.08}^{+0.12})\%$ of the decay rate, smaller than our statistical uncertainty in our $\phi e \nu_e$ branching fraction. We also look for $\pi\pi$, KK , and $K\pi$ outside the mass windows corresponding to the resonant states studied and we found no evidence for additional channels.

We consider several sources of systematic uncertainty. The dominant component is associated with the number of tags, which is affected by the lack of our knowledge on the random γ in the background PDFs. We estimate it by repeating the fit with a variety of shapes, namely, polynomials of different order, or special shapes derived from MC simulation, and obtain an uncertainty of 3.6%. Systematic uncertainties associated with hadron selection such as tracking (0.3% per charged particle), K and π identification (0.6% and 0.3%, respectively), and η selection criteria (2%) have been studied extensively [23]. Similarly, the K_S^0 selection criteria are derived from Ref. [24], and have (0.8%) uncertainty. The systematic uncertainty on the electron identification efficiency (1%) is assessed by comparing radiative Bhabha samples, Bhabha events embedded in hadronic events, and MC samples. The requirements that there are no extra tracks in the event and that the net charge is zero have been evaluated with a data sample comprised of two hadronic tags. The comparison between results obtained with this sample and corresponding MC samples give an overall systematic uncertainty of 0.6% from these two requirements. Finally, we consider the dependence of the efficiency for semileptonic decays on the form factors. The CLEO MC uses the form factors predicted by the ISGW2 model [2]. We have generated also samples based on simple pole form factors and compared the efficiencies derived with the two methods to estimate this effect. The related systematic uncertainty ranges from 0.1% to 2.4%.

We check the normalization of our branching fractions by measuring the well known branching fraction $\mathcal{B}(D^0 \rightarrow K^- e^+ \nu_e)$ using a $D^- D^{*+}$ sample from the same data set.

We reconstruct $DD^* \rightarrow D^- D^{*+} \rightarrow D^- \pi^+ D^0$ decays, where the D^0 decays into $K^- e^+ \nu_e$, and the D^- decays into these six hadronic exclusive final states: $D^- \rightarrow K^+ \pi^- \pi^-$, $D^- \rightarrow K^+ \pi^- \pi^- \pi^0$, $D^- \rightarrow K_S^0 \pi^-$, $D^- \rightarrow K_S^0 \pi^- \pi^0$, $D^- \rightarrow K_S^0 \pi^- \pi^+ \pi^-$, $D^- \rightarrow K^+ K^- \pi^-$. The selection criteria and analysis procedure are the same as used in reconstructing the D_s semileptonic decays. We get in total 14759 ± 203 of tagged events and 350 ± 18 signal events, and using Eq. (4), we derive a branching fraction $\mathcal{B}(D^0 \rightarrow K^- e^+ \nu_e) = (3.45 \pm 0.21)\%$.

This result is in agreement with the two most recent absolute measurements: $\mathcal{B}(D^0 \rightarrow K^- e^+ \nu_e) = (3.61 \pm 0.05 \pm 0.05)\%$ from CLEO-c [25], based on 281 pb^{-1} data at the $\psi(3770)$, and $\mathcal{B}(D^0 \rightarrow K^- e^+ \nu_e) = (3.45 \pm 0.07 \pm 0.20)\%$ from Belle [26].

All the measurements reported here are first absolute measurements of exclusive semileptonic D_s decays, moreover this is the first report of Cabibbo suppressed final states and scalar meson above the threshold to decay in the observed final state. For the six D_s semileptonic decays considered, Table III shows the derived branching fractions including the systematic errors.

These results allow us to draw several interesting conclusions. The sum of the branching fractions measured imply $\mathcal{B}(D_s^+ \rightarrow X e^+ \nu_e) = (6.47 \pm 0.60)\%$, about 16% below the value $(7.82 \pm 0.13)\%$, inferred from measured D^+ and D_z inclusive semileptonic branching fraction [27] and the charmed meson lifetimes [21]. We have searched for additional hadronic final states formed with two charged tracks, as well as from two charged tracks and a π^0 , and found no evidence for semileptonic decays including other hadronic final states. No other significant branching fraction is expected. This result is consistent with the predictions of the ISGW2 model [2], supporting the conjecture that SU(3) is broken in charm semileptonic decays.

TABLE III. The derived branching fractions including the systematic errors for the six semileptonic channels studied. The $D_s^+ \rightarrow f_0 e^+ \nu_e$ branching fraction quoted represents the product branching fraction $\mathcal{B}(D_s^+ \rightarrow f_0 e^+ \nu_e) \times \mathcal{B}(f_0 \rightarrow \pi^+ \pi^-)$, which is the dominant decay mode in Ref. [21].

Signal Mode	\mathcal{B} (%)
$D_s^+ \rightarrow \phi e^+ \nu_e$	$2.29 \pm 0.37 \pm 0.11$
$D_s^+ \rightarrow \eta e^+ \nu_e$	$2.48 \pm 0.29 \pm 0.13$
$D_s^+ \rightarrow \eta' e^+ \nu_e$	$0.91 \pm 0.33 \pm 0.05$
$D_s^+ \rightarrow K^0 e^+ \nu_e$	$0.37 \pm 0.10 \pm 0.02$
$D_s^+ \rightarrow K^{*0} e^+ \nu_e$	$0.18 \pm 0.07 \pm 0.01$
$D_s^+ \rightarrow f_0 e^+ \nu_e$	$0.13 \pm 0.04 \pm 0.01$

On the other hand, the difference in widths may arise from nonfactorizable contributions at the level of $\sim 10\%$ [1]. The ratio $\mathcal{B}(D_s^+ \rightarrow \eta' e^+ \nu_e) / \mathcal{B}(D_s^+ \rightarrow \eta e^+ \nu_e) = 0.36 \pm 0.14$, is in agreement with the previous CLEO result [15]. The ISGW2 model involves a η/η' mixing angle close to -10° , which is the minimum value obtained from mass formulas [21] if a quadratic approximation is used. According to Ref. [5], the measured ratio is consistent with a pseudoscalar mixing angle of about -17° , provided that a glueball component probability of the order of 10% is present in the η' . Finally, we have the first measurement of a D_s semileptonic decay including a scalar meson above the threshold for decay to the observed final state, which opens up the exciting possibility of elucidating the nature of exotic light mesons [6].

We gratefully acknowledge the effort of the CESR staff in providing us with excellent luminosity and running conditions. This work was supported by the National Science Foundation and the U.S. Department of Energy.

-
- [1] M. B. Voloshin, Phys. Lett. B **515**, 74 (2001).
[2] D. Scora and N. Isgur, Phys. Rev. D **52**, 2783 (1995).
[3] N. E. Adam *et al.* (CLEO Collaboration), Phys. Rev. Lett. **97**, 251801 (2006).
[4] M. S. Witherell, AIP Conf. Proc. **302**, 198 (1994).
[5] V. V. Anisovich, D. V. Bugg, D. I. Melikhov, and V. A. Nikonov, Phys. Lett. B **404**, 166 (1997).
[6] H. G. Dosch and S. Narison, Nucl. Phys. B, Proc. Suppl. **121**, 114 (2003).
[7] A. H. Fariborz, R. Jora, and J. Schechter, Nucl. Phys. B, Proc. Suppl. **186**, 298 (2009).
[8] J. M. Link *et al.*, (FOCUS Collaboration), Phys. Lett. B **541**, 243 (2002).
[9] F. Butler *et al.* (CLEO Collaboration), Phys. Lett. B **324**, 255 (1994).
[10] P. L. Frabetti *et al.*, Phys. Lett. B **313**, 253 (1993).
[11] H. Albrecht *et al.* (ARGUS Collaboration), Phys. Lett. B **245**, 315 (1990).
[12] J. P. Alexander *et al.* (CLEO Collaboration), Phys. Rev. Lett. **65**, 1531 (1990).
[13] J. P. Alexander *et al.* (CLEO Collaboration), Phys. Rev. Lett. **100**, 161804 (2008).
[14] B. Aubert *et al.* (BABAR Collaboration), Phys. Rev. D **78**, 051101 (2008).
[15] G. Brandenburg *et al.* (CLEO Collaboration), Phys. Rev. Lett. **75**, 3804 (1995).
[16] J. Z. Bai *et al.* (BES Collaboration), Phys. Rev. D **56**, 3779 (1997).
[17] Y. Kubota *et al.*, Nucl. Instrum. Methods Phys. Res., Sect. A **320**, 66 (1992).
[18] D. Peterson *et al.*, Nucl. Instrum. Methods Phys. Res., Sect. A **478**, 142 (2002).

- [19] M. Artuso *et al.*, Nucl. Instrum. Methods Phys. Res., Sect. A **502**, 91 (2003).
- [20] D. Cronin-Hennessy *et al.* (CLEO Collaboration), arXiv:0801.3418.
- [21] W.M. Yao *et al.* (Particle Data Group), J. Phys. G **33**, 1 (2006).
- [22] T.E. Coan *et al.* (CLEO Collaboration), Phys. Rev. Lett. **95**, 181802 (2005).
- [23] S. Dobbs *et al.* (CLEO Collaboration), Phys. Rev. D **76**, 112001 (2007).
- [24] J.L. Rosner *et al.* (CLEO Collaboration), Phys. Rev. Lett. **100**, 221801 (2008).
- [25] J.Y. Ge *et al.* (CLEO Collaboration), Phys. Rev. D **79**, 052010 (2009).
- [26] L. Widhalm, Phys. Rev. Lett. **97**, 061804 (2006).
- [27] N.E. Adam *et al.* (CLEO Collaboration), Phys. Rev. Lett. **97**, 251801 (2006).